Role of cantharidin in the activation of IKKα/IκBα/NF-κB pathway by inhibiting PP2A activity in cholangiocarcinoma cell lines

HUIJIANG ZHOU[1,2], JIANGFENG XU[1], SHUAI WANG[1] and JINFENG PENG[1]

[1]Department of General Surgery, The Fourth Affiliated Hospital,
Zhejiang University School of Medicine, Yiwu, Zhejiang 322000; [2]Department of General Surgery,
Sir Run Run Shaw Hospital, Zhejiang University School of Medicine, Hangzhou, Zhejiang 310016, P.R. China

Abstract. Cantharidin (CAN), a potent inhibitor of serine/threonine-protein phosphatase 2A (PP2A), is widely used in clinical practice, particularly in the treatment of advanced cancer due to its specific action on these types of cancer. In the present study, the inhibitory effect of CAN was examined in two cholangiocarcinoma cell lines (QBC939 and Hucc-t1). Following treatment with CAN, cell viability was effectively reduced in QBC939 and Hucc-t1 cells and normal human intrahepatic biliary epithelial cells. However, a slight increase in reactive oxygen species levels in QBC939 cells treated with CAN was observed post-treatment. CAN significantly inhibited cell migration and invasion in a dose-dependent manner. Western blot analysis demonstrated that the nuclear factor-κB (NF-κB) pathway was stimulated by CAN, which was confirmed by the upregulated phosphorylation levels of inhibitor of NF-κB kinase subunit α (IKKα) and NF-κB inhibitor α (IκBα) in cells, and an increased NF-κB p65 subunit level in the nucleus. The expression levels of 72 kDa type IV collagenase (MMP2) and matrix metalloproteinase 9 (MMP9) were downregulated by CAN. Notably, there was a negative association between MMP2 and MMP9 expression levels, and NF-κB p65, although NF-κB p65 regulates the expression of MMP2 and MMP9 and has a positive association with these proteins in various types of cancer. Notably, it was observed that CAN exerted specific inhibition on PP2A activity and thereby resulted in the activation of the IKKα/IκBα/NF-κB pathway. Therefore, CAN-induced cell inhibition maybe partially dependent on the activation of the IKKα/IκBα/NF-κB pathway. In conclusion, it was demonstrated that CAN selectively and effectively inhibited cholangiocarcinoma cell migration and invasion. The present study may provide a novel insight into the use of CAN as a therapeutic candidate in the treatment of cholangiocarcinoma.

Introduction

Cholangiocarcinoma (CC) is a malignant tumor originating from biliary epithelia within intrahepatic and extrahepatic tracts (1,2). Although the incidence of CC is rare globally, its prevalence and mortality rate is growing annually (2). The challenges put forward by this cancer are hardly diagnosed early for its ease of migration and perineural invasion (3). The only present treatment for long-term survival for patients with CC is surgical resection (4,5). However, the recurrence rate of this cancer following surgery is high and current chemotherapy practices have not been able to increase the survival rate of this cancer (4,6). Alterations in apoptotic thresholds induced by a chronic inflammatory state are an important indicator during the development of CC (7).

Primary sclerosing cholangitis and primary biliary cirrhosis are the important risk factors for CC (8-10). The inflammatory environment in these conditions leads to further cell damage, inducing dysregulation of apoptosis (10).

Recently, regarding the multivariate and multi-stage processes of cancer, interfering with or inhibiting one or several factors leading to these processes is an effective method of preventing, or providing therapy for cancer (11). However, in order to inhibit these processes, effective molecular targets are required. According to epidemiological investigations, nuclear factor kappa B (NF-κB) is a widely distributed and important transcription factor participating in various biological processes, including immune responses, inflammatory reactions, apoptosis, tumorigenesis and tumor proliferation (12,13). Activation of NF-κB-mediated gene transcription, including viral proteins, cell mitogens and tumor necrosis factor-α, is stimulated by a variety of factors (14). The majority of the cytoplasmic form of NF-κB was associated with the members of the inhibitor of NF-κB family, including NF-κB inhibitor α

Correspondence to: Dr Huijiang Zhou, Department of General Surgery, The Fourth Affiliated Hospital, Zhejiang University School of Medicine, N1 Shangcheng Road, Yiwu, Zhejiang 322000, P.R. China
E-mail: 3307013@zju.edu.cn

(IκBα). NF-κB is released when IκBα is phosphorylated by cellular stimulation, and is translocated to the nucleus where it stimulates the transcription of genes that have an NF-κB binding site (14,15).

It is well known that IκB kinases (IKK), RAC-α serine/threonine-protein kinase (AKT), mitogen-activated protein kinase and casein kinase II are regulated by serine/threonine-protein phosphatase 2A (PP2A), a serine-threonine phosphatase family member involved in the cell cycle, metabolism, cell growth, transcription, translation and apoptosis (16,17). PP2A holoenzymes consist of a structural subunit A, a regulatory subunit B and a catalytic subunit C (17). Previous investigations demonstrated that cantharidin (CAN), derived from cantharis, which has been widely used in traditional Chinese medicine, is a strong inhibitor of PP2A (18,19). CAN and its derivatives have a marked effect on the inhibition of various types of cancer, including gallbladder carcinoma, bladder cancer, leukemia and hepatoma (17,18). Clinical applications have indicated that CAN exhibits unique efficacy in cancer treatment, particularly for advanced liver cancer, by increasing leukocyte numbers (20).

The majority of cases of CC are diagnosed at an advanced stage (21). Therefore, CAN may be used for the treatment of CC due to its specific efficacy in advanced cancer, and it is necessary to investigate its molecular mechanisms. In addition, a previous study revealed that the inhibitory effects of CAN in cancer may involve the inhibition of cellular migration and invasion (22). The aim of the present study was to examine the precise molecular mechanisms inducing the inhibitory effect of CAN on the migration and invasion of a CC cell line. The present study suggested that CAN may inhibit cellular migration and invasion in QBC939 cells by stimulating the IKKα/IκBα/NF-κB signaling pathway, and by regulating the expression of proteins associated with cellular migration and invasion, including metalloproteinase inhibitors (TIMPs) and matrix metalloproteinases (MMPs).

Materials and methods

Cell culture. Human cholangiocarcinoma cell lines QBC939 and Hucc-t1, as well as human intrahepatic biliary epithelial cells (HiBECs) were obtained from the Cell Bank of the Type Culture Collection of the Chinese Academy of Sciences (Shanghai, China) and ScienCell Research Laboratories, Inc. (San Diego, CA, USA), respectively. QBC939, Hucc-t1 and HiBECs were cultured in RPMI-1640 medium (Gibco; Thermo Fisher Scientific, Inc., Waltham, MA, USA) containing 10% fetal bovine serum (FBS; Gibco; Thermo Fisher Scientific, Inc.) and antibiotics, at 37˚C under a humidified atmosphere with 5% CO_2 and 95% air.

Cell viability assay. QBC939 cells and HiBECs were incubated in CAN (Biomol; Enzo Life Sciences, Inc., Farmingdale, NY, USA) at 3, 6, 10, 20 and 40 μM, as well as the p65 inhibitor caffeic acid phenethyl ester (CAPE; 1 μM), the PP2A inhibitor okadaic acid (OA; 1 nM) or the PP2A activator D-erythro-sphingosine (DES; 10 nM) for 12, 24, 48 and 72 h. Thereafter the cytotoxic or anti-proliferative effect of CAN was investigated using a MTT assay (Roche Applied Science,

Penzberg, Germany), according to the manufacturer's protocol. The precipitated formazan was dissolved in 150 μl dimethyl sulfoxide and the wavelength used to measure the formazan was 570 nm.

PP2A activity assay. QBC939 cells (1x10^4) and HiBECs (1x10^4) were incubated with CAN at 6 and 10 μM for 6, 12, 24, 48 h, followed by treatment with the PP2A inhibitor okadaic acid (OA; 1 nM) or the PP2A activator D-erythro-sphingosine (DES; 10 nM) for 24 h at 37˚C. The activity of PP2A was subsequently measured with a nonradioactive serine/threonine-phosphatase assay kit (Promega Corporation, Madison, WI, USA), according to the manufacturer's protocol. Cell lysate was removed by a Sephadex G-25 column twice and was seeded on a 96-well plate, the reaction substrate of PP2A, RRA(pT)VA, was added (23), and was incubated with molybdate dye at 25˚C for 30 min. Plates were read using a SpectraMax® M5/M5e (Molecular Devices LLC, Sunnyvale, CA, USA) at 630 nm. The relative activity of PP2A was expressed as the percentage of QBC939- and HiBEC-positive cells.

Cell experiments. QBC939 cells grown to 90% confluency were incubated with CAN at 0 (control), 2, 6 and 10 μM for 24 h, and subsequently harvested for the following assays.

Reactive oxygen species (ROS) assay. Cells (1x10^5) incubated with CAN were collected and washed with PBS. Subsequently, cells were incubated in a solution containing 10 μM dichloro-dihydro-fluorescein diacetate (Sigma-Aldrich; Merck KGaA, Darmstadt, Germany) at 37˚C for 1 h. Cells were washed three times. ROS production was determined by flow cytometry by measuring the alterations in fluorescence (emission, 510 nm; excitation, 488 nm).

Transwell cell migration assay. In a sterile environment, cells were detached from the plate using 0.25% trypsin-EDTA solution, harvested following centrifugation at 500 x g for 5 min at 4˚C, and washed twice to remove the serum. Cells resuspended with Dulbecco's modified Eagle's medium (DMEM, Gibco; Thermo Fisher Scientific, Inc.) were adjusted to 1x10^6 cells/ml, and 300 μl cell solution was added to the top chamber of the Transwell (BD Biosciences, Franklin Lakes, NJ, USA) and placed on a 24-well plate for 2 h at 37˚C. Finally, 500 μl DMEM containing 2.5% FBS was added to the bottom chamber of the Transwell and incubated for 24 h at 37˚C. Following incubation, the migratory cells were fixed and stained with 0.1% crystal violet dye for 20 min at room temperature. Following dissolving in 200 μl 33% acetic acid, the absorbance value at 570 nm was read with the Spectra Max® M5/M5e. The migration rate was calculated as a percentage of the control.

Transwell cell invasion assay. Cells were harvested as previously described, resuspended with DMEM and adjusted to 1x10^6 cells/ml. Cell migration was determined using the ECM554 invasion kit (Chemicon; EMD Millipore, Billerica, MA, USA), according to the manufacturer's protocol. The top chamber of the Transwell was placed on a 24 well plate and 300 μl serum free medium was added, and DMEM medium
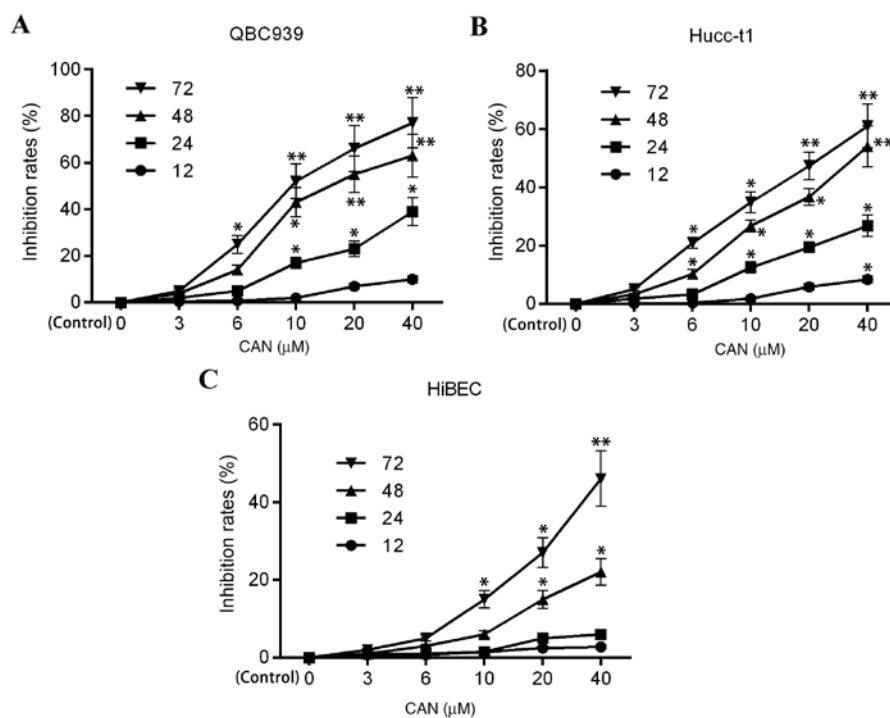
Figure 1. CAN exerts significant inhibition on cell viability in human cholangiocarcinoma cells. CAN increased the inhibition rates of (A) QBC939 and (B) Hucc-t1 cells in a dose and time dependent manner, as measured by MTT assay. (C) Compared with QBC939 and Hucc-t1 cells, HiBECs were more tolerant to the cytotoxicity of CAN. Data are expressed as the mean ± standard deviation. $^{*}P<0.05$, $^{**}P<0.01$ vs. control (0 μM). CAN, cantharidin; HiBECs, human intrahepatic biliary epithelial cells.

containing 2.5% FBS was added into the bottom chamber. Following incubation for 10 min at 37°C, 250 μl DMEM in the top chamber was replaced with 250 μl cell solution and incubated for 24 h at 37°C. The invaded cells were stained using 0.1% crystal violet dye for 20 min at room temperature. The number of invaded cells was counted under an inverted microscope at a magnification of x200. The invasion rate was expressed as a percentage of the control.

Western blot assay. QBC939 cells were incubated in CAN at 3, 6, 10, 20 and 40 μM, as well as CAPE (1 μM), OA (1 nM) for 12, 24, 48 and 72 h. Following this, cells were harvested and washed with ice-cold PBS, and solubilized in lysis buffer containing protease inhibitors (Sigma-Aldrich; Merck KGaA). Total protein was extracted and measured using a bicincho- ninic acid protein assay kit (Pierce; Thermo Fisher Scientific, Inc.), following the manufacturer's protocol. Nucleoprotein was extracted using NE-PER Nuclear and Cytoplasmic Extraction reagent (Pierce; Thermo Fisher Scientific, Inc.) according to the manufacturer's protocol. Protein (50 μg/lane) was separated by 10% SDS-PAGE and subsequently trans- ferred to polyvinylidene fluoride membranes (Bio-Rad Laboratories, Inc., Hercules, CA, USA). Following blocking in 5% non-fat dry milk for 1 h at room temperature, the membranes were incubated with primary antibodies at 4°C overnight. The protein level was measured using a horseradish peroxidase-conjugated secondary antibody (cat no. P0162; 1:100; Dako, Agilent Technologies, Inc., Santa Clara, CA, USA) for 1 h at room temperature. Blots were developed using an enhanced chemiluminescence detection kit from Amersham (GE Healthcare, Chicago, IL, USA). The primary

antibodies were as follows: NF-κB/p65 (cat no. D14E12; 1:1,000), phosphorylated (p-)IKKα (cat no. C84E11; 1:1,000), IKKα (cat no. 3G12; 1:1,000), p-IκBα (cat no. 5A5; 1:1,000), IκBα (cat no. L35A5; 1:1,000), β-actin (cat no. D6A8; 1:1,000), PP2A (cat no. 52F8; 1:1,000), p-p65 (cat no. 93H1; 1:1,000), MMP-9 (cat no. D6O3H; 1:1,000), MMP-2 (cat no. D4M2N; 1:1,000), TIMP-1 (cat no. D10E6; 1:1,000), TIMP-2 (cat no. D18B7; 1:1,000) and Lamin B (cat no. D9V6H; 1:1,000; all CST Biological Reagents Co., Ltd., Shanghai, China). β-actin was used as the internal control.

Reverse transcription-quantitative polymerase chain reac- tion (RT-qPCR) assay. Total RNA was isolated from cells using a commercially available RNeasy mini-kit (Qiagen, Inc., Valencia, CA, USA), according to the manufacturer's protocol. Total RNA (1 μg) was reverse transcribed using an NCode VILO miRNA cDNA Synthesis kit (Invitrogen; Thermo Fisher Scientific, Inc.), according to the manu- facturer's protocol. The primer sequences for RT-qPCR were purchased from Integrated DNA Technologies, Inc. (Coralville, IA, USA). Quantification of relative mRNA was performed using iQ SYBR-Green Supermix on the iCycler iQ thermal cycler (Bio-Rad Laboratories, Inc.). The ther- mocycling conditions for qPCR were as follows: 45°C for 10 min, 95°C for 10 min, followed by 50 cycles of 95°C for 15 sec and 60°C for 45 sec. The amplification products of the PCR were verified by melting curve analysis. Results were calculated using the $\Delta\Delta$Cq method (24). Relative expres- sion of mRNA was normalized to β-actin expression levels. Primers were as follows: MMP-2 forward, 5'-GGCCGTGTT TGCCATCTGTT-3' and reverse, 5'-TGCAGGGAGCAG
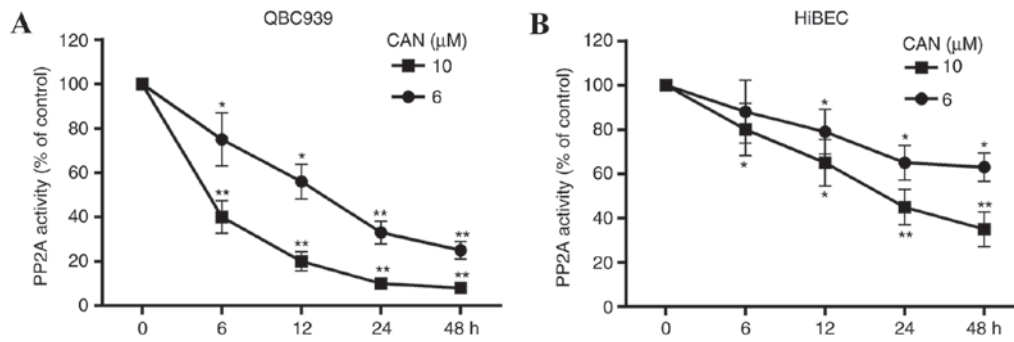
Figure 2. PP2A activity is inhibited in QBC939 cells and HiBECs following treatment with CAN. PP2A activity in (A) QBC939 cells and (B) HiBECs was decreased upon treatment with CAN, in a time- and dose-dependent manner. Data are expressed as the mean ± standard deviation. *P<0.05, **P<0.01 vs. control (0 μM). CAN, cantharidin; PP2A, serine/threonine-protein phosphatase 2A.
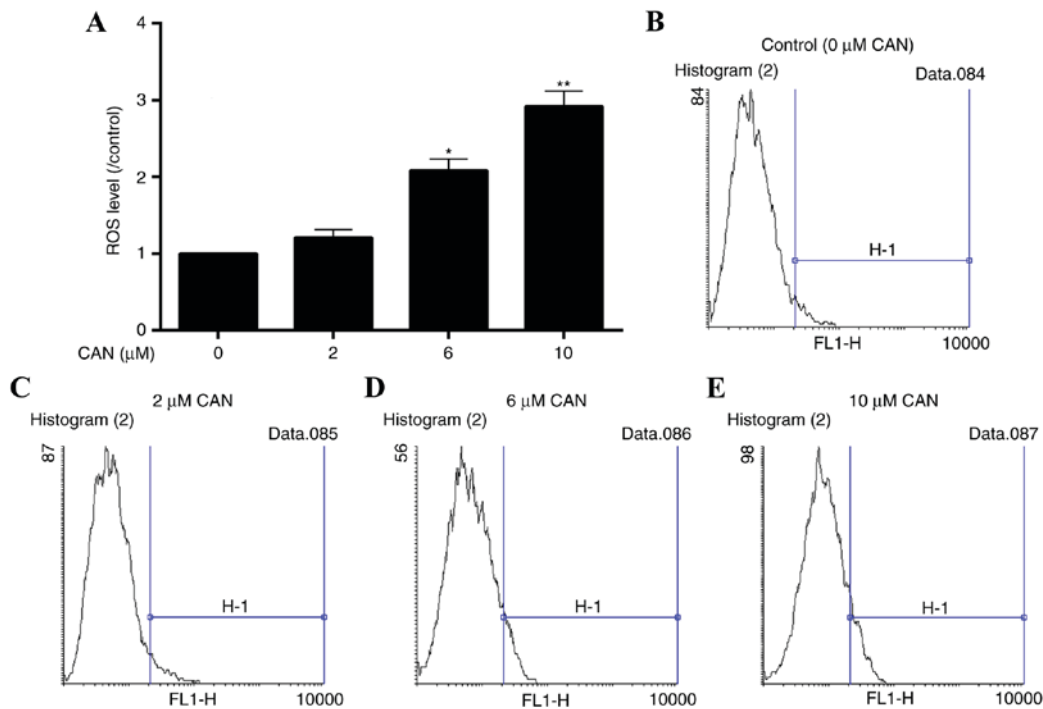

Figure 3. ROS levels in QBC939 are increased following treatment with CAN. (A) Quantification of ROS levels in cells, as measured with flow cytometry following treatment with (B) 0 μM (control), (C) 2 μM, (D) 6 μM and (E) 10 μM CAN for 24 h. Data are expressed as the mean ± standard deviation. *P<0.05, **P<0.01 vs. control. CAN, cantharidin; ROS, reactive oxygen species.

AGATTCGG-3'; MMP-9 forward, 5'-CCAGTCCACCCT TGTGCTCT-3' and reverse, 5'-CTCTCCACGCATCTCTGC CA-3'; TIMP-2 forward, 5'-CGACTGGTCCAGCTCTGA CA-3' and reverse, 5'-TGGCAGAGGGAGGATGGGAT-3'; β-actin forward, 5'-GGCACTCTTCCAGCCTTCCT-3' and reverse, 5'-GCACTGTGTTGGCGTACAGG-3'.

Dual-luciferase reporter gene assay. The cells were seeded into 96-well plates at 70% confluence. After 16 h, cells were transfected with NF-κB luciferase reporter plasmid (Promega Corporation) and Lipofectamine® 2000 (Invitrogen; Thermo Fisher Scientific, Inc.). Following incubation for 48 h at 37℃, cells were collected to measure the luciferase activity with the Dual-Luciferase Reporter Assay System kit (Promega Corporation). The transcriptional activities of genes were expressed as the ratio between firefly luciferase and *Renilla* luciferase.

Statistical analysis. Data are expressed as the mean ± standard deviation. Results were analyzed by two-tailed and unpaired Student's t-test. Multiple comparisons between three or more groups were performed using one-way analysis of variance, followed by Tukey's post-hoc test. SPSS 22.0 software (IBM Corp., Armonk, NY, USA) was used to perform the statistical analysis. P<0.05 was considered to indicate a statistically significant difference.

Results

CAN inhibits the viability of human cholangiocarcinoma cell lines. Fig. 1 illustrates the cell viability of CAN-treated human cholangiocarcinoma QBC939, Hucc-t1 and HiBECs, as demonstrated by MTT assay. The profiles of the inhibition rates of QBC939, Hucc-t1 and HiBECs following treatment with CAN were dose- and time-dependent. However, the
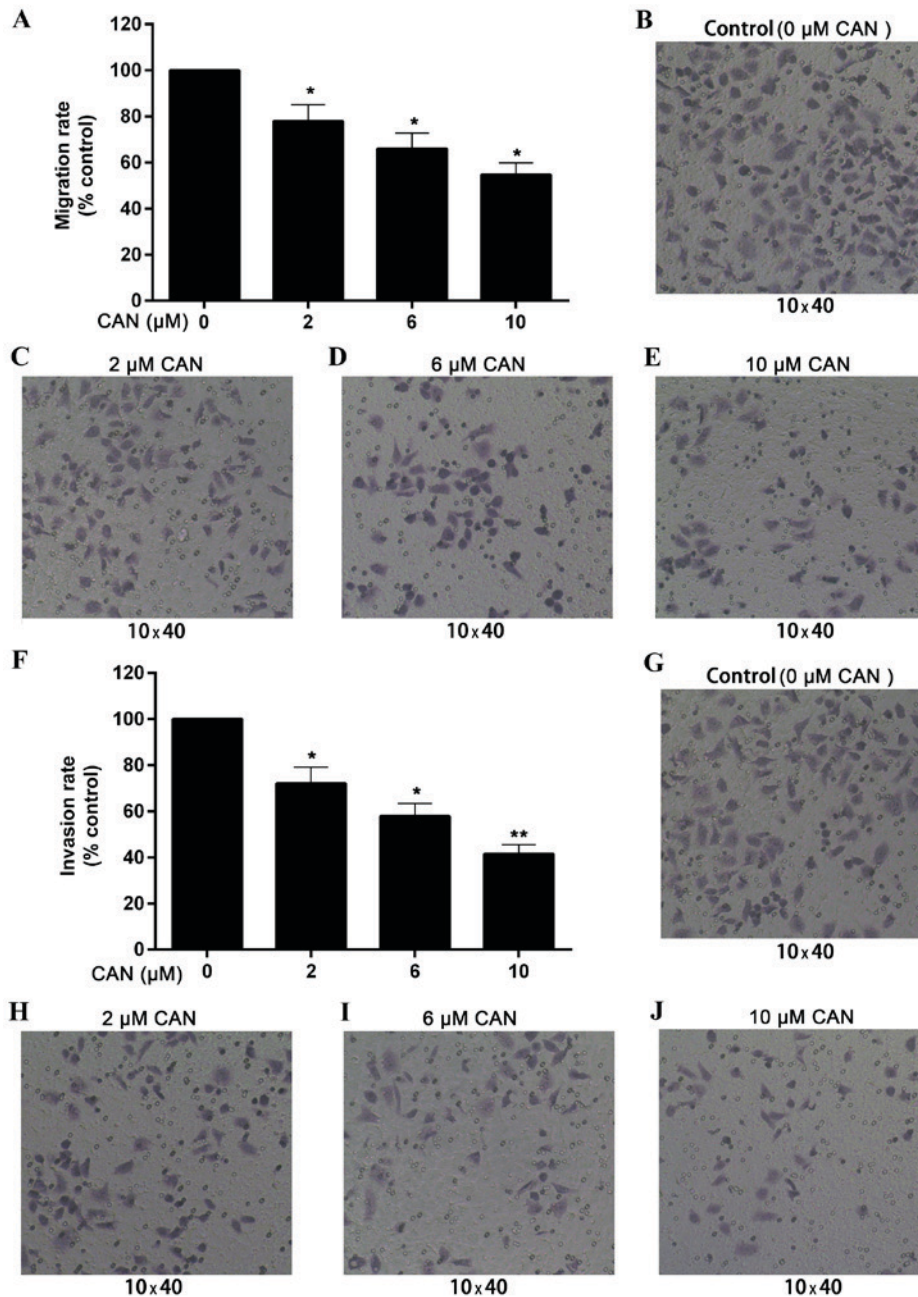
Figure 4. Migration and invasion of QBC939 cells is significantly inhibited following treatment with CAN. Quantification of (A) the migration activity of cells following treatment with (B) 0, (C) 2, (D) 6 and (E) 10 µM CAN for 24 h, as measured by Transwell cell migration assay; and of (F) the invasion activity of cells following treatment with (G) 0, (H) 2, (I) 6 and (J) 10 µM CAN for 24 h, as measured by Transwell cell invasion assay. Magnification, x400. Data are expressed as the mean ± standard deviation. *P<0.05, **P<0.01 vs. control. CAN, cantharidin.

inhibition rates in QBC939 and Hucc-t1 cells following treatment with CAN were significant increased compared with HiBECs, which indicated increased cytotoxicity of CAN inhuman cholangiocarcinoma cell lines compared with the normal HiBECs.

CAN inhibits the activity of PP2A. The effect of treatment with CAN (6 or 10 µM for 6, 12, 24 and 48 h) on the activity of PP2A in cells was determined. As presented in Fig. 2, PP2A activity was decreased in QBC939 cells and HiBECs following treatment with CAN. Compared with the HiBECs, increased inhibition of PP2A activity by CAN in QBC939 cells was observed. Additionally, PP2A activity was significantly

inhibited in HiBECs with CAN treatment at 10 mM for 24 and 48 h (Fig. 2B).

ROS levels in QBC939 are significantly increased following treatment with CAN for 24 h. To assess the oxidative damage in QBC939 cells induced by CAN, alterations in ROS levels in cells were determined. Following incubation with CAN at 0, 2, 6 and 10 µM for 24 h, ROS levels were elevated at all levels of treatment, compared with the control (0 µM; Fig. 3).

CAN effectively inhibits the migration and invasion of QBC939. Transwell cell migration and invasion assays were performed to assess the effect of CAN on the growth of
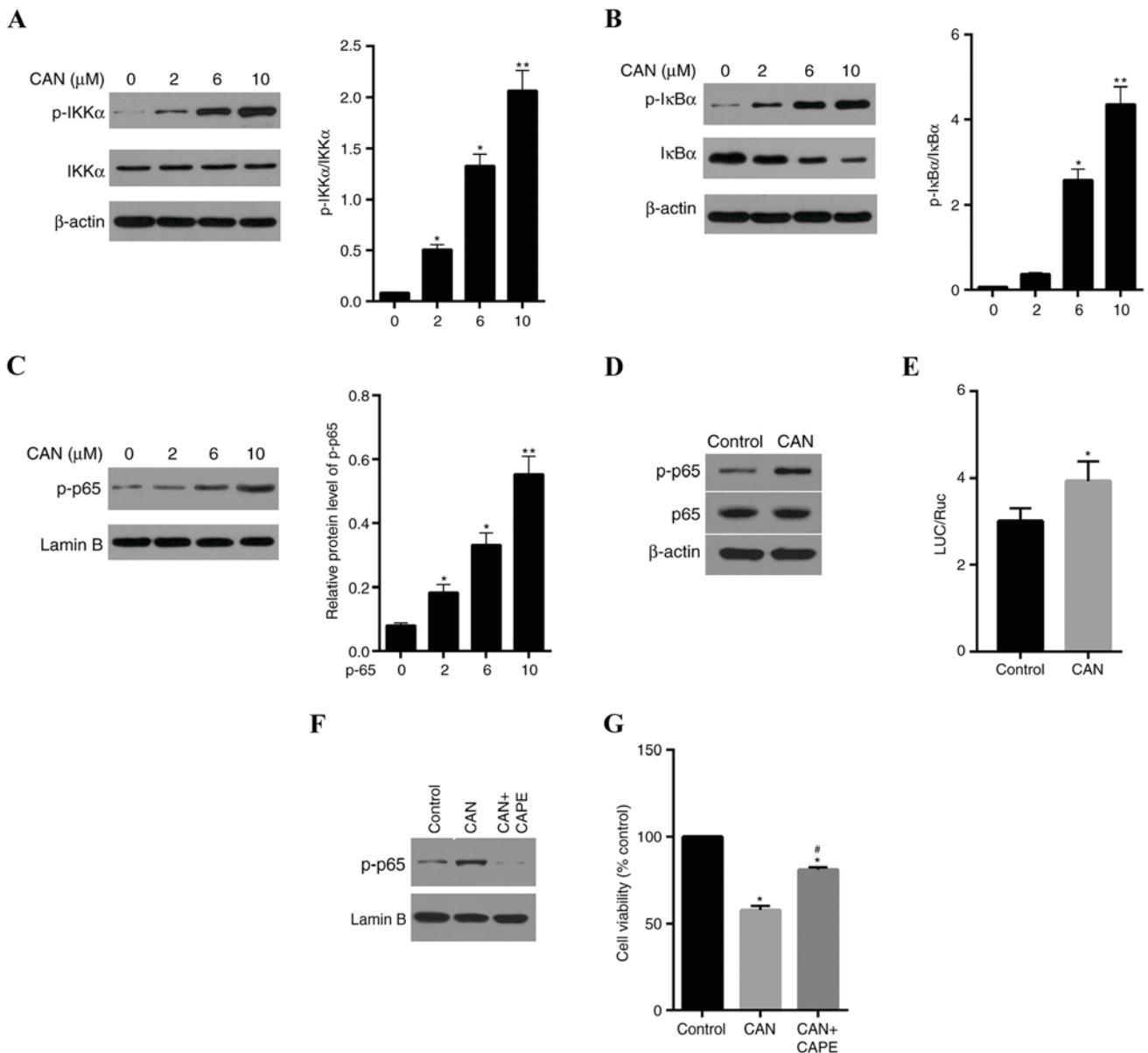
Figure 5. CAN-induced proliferation inhibition in QBC939 cells involves the activation of the NF-κB pathway. (A) p-IKKα levels in QBC939 cells were elevated following treatment with CAN, in a dose-dependent manner, compared with the control (0 µM). (B) p-IκBα and IκBα levels in cells were significantly increased and decreased, respectively, compared with the control, following treatment with CAN. (C) p-p65 levels in the nucleus were increased by treatment with CAN. (D) CAN increased p-p65 levels, although it had a weak impact on the total p65 protein expression. (E) The dual-luciferase reporter gene assay indicated that CAN may stimulate NF-κB(p65) transcriptional activity. (F) CAPE (1 µM), a specific inhibitor of p65, reduced the CAN-induced nuclear translocation of p-p65 and (G) partially decreased the cytotoxicity of CAN. Data are expressed as the mean ± standard deviation. *P<0.05, **P<0.01 vs. control; #P<0.05, CAN+CAPE vs. CAN. CAN, cantharidin; CAPE, caffeic acid phenethyl ester; NF-κB, nuclear factor-κB; IKK, inhibitor of NF-κB kinase; LUC, luciferase; p, phosphorylated; IκBα, NF-κB inhibitor α; Ruc, *Renilla* luciferase.

QBC939. As presented in Fig. 4A-E, QBC939 migration was reduced by CAN at 2, 6 and 10 µM for 24 h, compared with the control (without treatment). The migration rate of QBC939 cells was decreased to 54.7% of that of the control following treatment with 10 µM for 24 h.

Similarly, the invasion rate was significantly reduced by treatment with CAN for 24 h and appeared to be dose-dependent. As presented in Fig. 4F-J, the relative invasion rates in cells following treatment with 2, 6 and 10 µM CAN for 24 h were 72.1, 57.8 and 41.5%, respectively, compared with the control.

CAN-induced cell inhibition is partially dependent on the IKKα/IκBα/NF-κB signaling pathway. PP2A may deactivate IKKα by dephosphorylation of its active site, while IKKα is involved in the stimulation of the NF-κB pathway (25). Therefore, the activities of genes involved in the NF-κB signaling pathway in QBC939 cells was determined. As presented in Fig. 5A, p-IKKα levels were increased following treatment of cells with 2, 6, 10 µM CAN for 24 h, compared with the control. However, inhibition of PP2A by CAN exerted no apparent effects on the total IKKα levels. The expression levels of p-IκBα, the target protein of p-IKKα, were significantly elevated, and total IκBα levels were decreased when PP2A was inhibited by CAN, compared with the control (Fig. 5B). The levels of p65 in the nucleus was further determined. As illustrated in Fig. 5C, compared with the
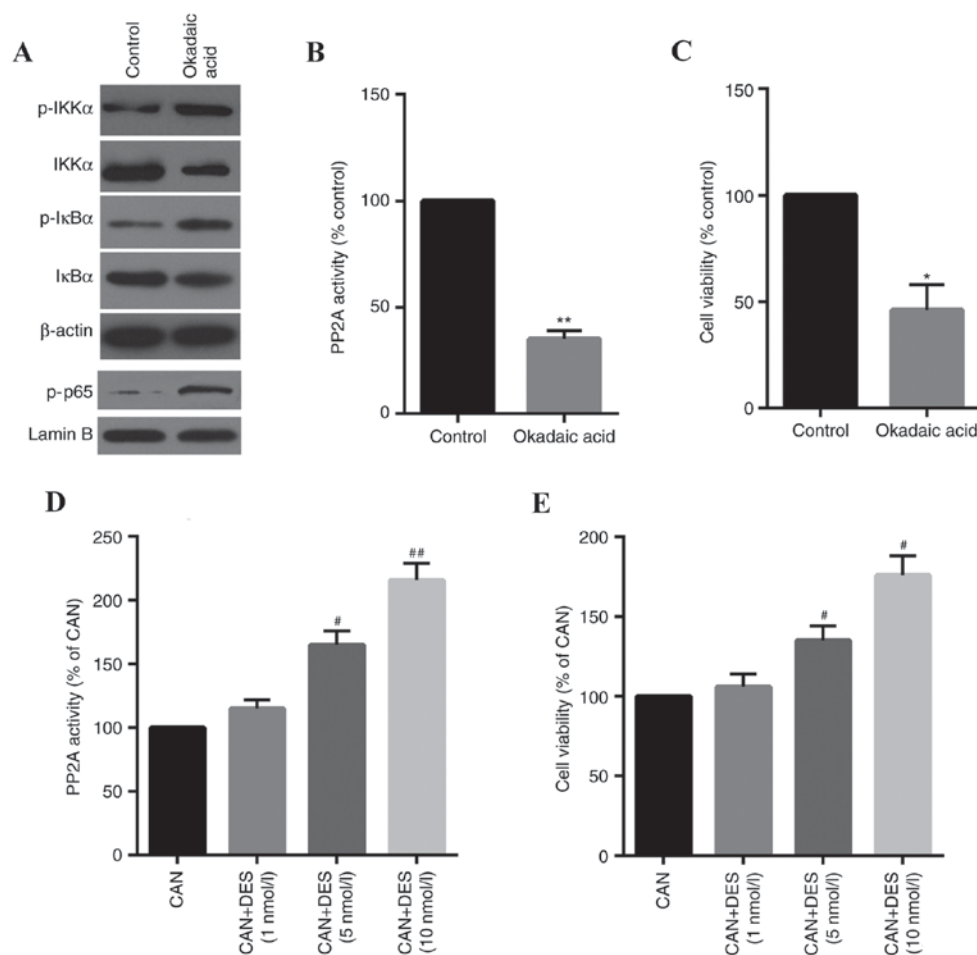
Figure 6. Specific inhibition of PP2A is involved in the CAN-induced proliferation of QBC939 cells. (A) The phosphorylation of IKKα/IκBα/NF-κB-associated proteins was increased by OA (1 nM), as measured by western blotting. (B) PP2A activity and (C) cell viability were suppressed in cells treated with OA. (D) PP2A activity and (E) cell viability were upregulated in a dose-dependent manner in cells treated with DES (10 nM), a specific activator of PP2A. Data are expressed as the mean ± standard deviation. *P<0.05, **P<0.01 vs. control; #P<0.05, ##P<0.01 vs. CAN. CAN, cantharidin; DES, D-erythro-sphingosine; NF-κB, nuclear factor-κB; IKK, inhibitor of NF-κB kinase; IκBα, NF-κB inhibitor α; OA, okadaic acid; p, phosphorylated; PP2A, serine/threonine-protein phosphatase 2A.

control, p65 levels were significantly increased in the nucleus following treatment with CAN. The phosphorylation of p65 and total p65 levels in cells treated with CAN (6 μM) was determined, and it was demonstrated that CAN increased the expression levels of p-P65 protein and had no marked impact on the expression of total p65 protein in cells (Fig. 5D). The dual-luciferase reporter gene assay revealed that CAN exerted light stimulation of the transcriptional activity of NF-κB (p65; Fig. 5E). To test whether CAN-induced cell inhibition is dependent on, partially dependent on or independent of the NF-κB pathway, the effect of CAPE, a specific inhibitor of p65, on nuclear p65 was further measured, and it was demonstrated that CAPE reversed CAN-induced nuclear translocation of p65 (Fig. 5F) and partially weakened the cytotoxicity of CAN (Fig. 5G).

CAN-induced stimulation of the IKKα/IκBα/NF-κB pathway is specifically involved in the inhibition of PP2A. To confirm the inhibition of PP2A on the IKKα/IκBα/NF-κB pathway in QBC939 cells, the effects of OA, a specific PP2A inhibitor, on cells were determined. The results indicated that the IKKα/IκBα/NF-κB pathway was activated by OA (Fig. 6A)

and PP2A activity and cell viability were inhibited in cells treated with OA (Fig. 6B and C). The role of PP2A in CAN-induced cell inhibition was further confirmed using DES, a specific activator of PP2A. As presented in Fig. 6D and E, PP2A activity and cell viability was increased in a dose-dependent manner.

Migration and invasion-associated genes are significantly altered at the translational and transcriptional levels following treatment with CAN. The expression of genes associated with migration and invasion, including MMP2, MMP9, TIMP-1 and TIMP-2, was examined (Fig. 7). The results demonstrated that the mRNA and protein expression levels of MMP2 and MMP9 were significantly downregulated when cells were treated with CAN compared with the control. By contrast, the expression levels of TIMP-1 and TIMP-2 mRNA and protein in cells were increased in a dose-dependent manner following treatment with CAN, compared with the control. The dual-luciferase reporter gene assay revealed that the transcriptional activities were downregulated for MMP2 and MMP9 and were upregulated for TIMP-1 and TIMP-2 in cells treated with CAN compared with the control (Fig. 7C-F).
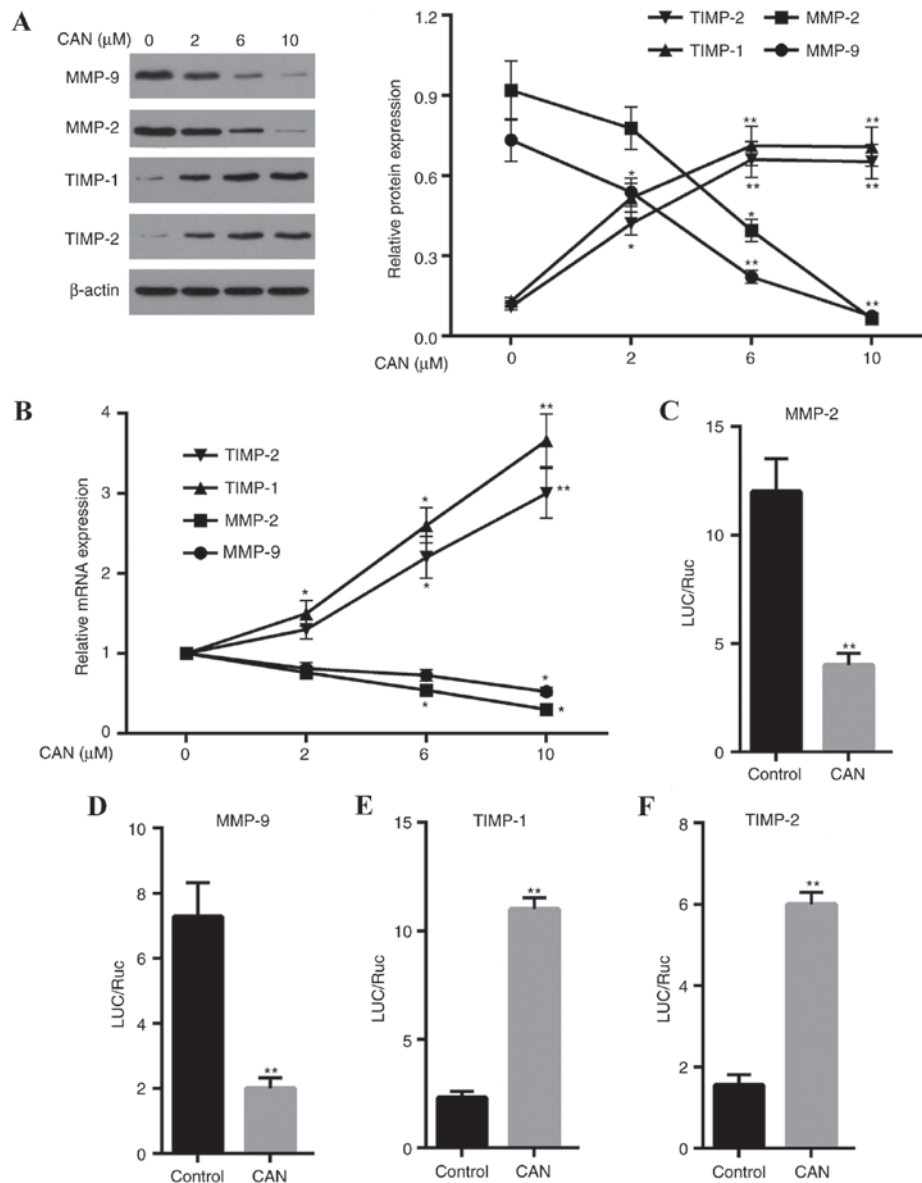
Figure 7. CAN inhibits the migration and invasion of QBC939 cells through upregulation of TIMP-1 and TIMP-2, and downregulation of MMP2 and MMP9. (A) MMP2 and MMP9 protein expression levels were decreased in QBC939 cells following treatment with CAN, whereas TIMP-1 and TIMP-2 protein expression levels were increased in QBC939 cells following treatment with CAN. (B) QBC939 cells treated with CAN exhibited reduced levels of MMP2 and MMP9 mRNA, while expression levels of TIMP-1 and TIMP-2 mRNA were increased. (C) The dual-luciferase reporter gene assay demonstrated that the transcriptional activities were decreased for MMP2 and (D) MMP9, and increased for (E) TIMP-1 and (F) TIMP-2, in cells treated with CAN. Data are expressed as the mean ± standard deviation. *P<0.05, **P<0.05 vs. control. CAN, cantharidin; LUC, luciferase; TIMP, metalloproteinase inhibitor; MMP2, 72 kDA type IV collagenase; MMP9, matrix metalloproteinase 9; Ruc, *Renilla* luciferase.

Discussion

Cholangiocarcinoma is a type of cancer with a high mortality rate, characterized by low survival rates, and is hardly diagnosed in the early phases (7,9). CAN is a product extracted from traditional Chinese medicine, serving an important role in the treatment of a variety of types of advanced cancer (18,22). In the present study, the action of CAN on cholangiocarcinoma QBC939 cells was determined.

Following treatment with CAN, the cell viability of QBC939 cells, Hucc-t1 cells and HiBECs was decreased, although it was demonstrated that HiBECs were less sensitive to CAN compared with QBC939 and Hucc-t1 cells. The activity of PP2A in cells treated with CAN was determined. The

results confirmed that CAN is a strong and specific inhibitor of PP2A in cholangiocarcinoma cells, since PP2A activity in HiBECs was increased compared with that in QBC939 cells. These results revealed that CAN exhibited higher efficiency in inhibiting QBC939 viability, and lower cytotoxicity was observed in normal HiBECs. Similarly, a number of reports have demonstrated that CAN and its derivatives have a selective inhibitory effect on cancer cells compared with normal cells (18,22,26). In addition, CAN derivatives, including synthetic cantharidin analogue, have decreased cytotoxicity in normal cells, supporting their application in the treatment of a variety of types of cancer (27).

ROS are the principal stimulator of cytotoxicity and an important factor causing oxidative damage (28,29). In the

present study, ROS levels were increased in a dose-dependent manner in cells treated with CAN. An efficient method of inhibiting the development of cancer is to reduce the migration and invasion of cancer cells (30). In the present study, the effect of CAN on the migration and invasion rates of QBC939 cells was determined. The results revealed that the migration and invasion rates were significantly decreased in a dose-dependent manner. Similarly, other studies proved that CAN has a marked inhibitory effect on the migration and invasion of cancer cells, including pancreatic cancer cells and liver cancer cells (18,31,32). These findings suggested that the inhibitory effect of CAN on cancer may involve inhibition of the migration and invasion of cancer cells.

PP2A is a pivotal protein phosphatase in cells and is involved in the phosphorylation of protein kinases, including IKK, glycogen synthase kinase-3β, protein kinase A, protein kinase C and RAC-α serine/threonine-protein kinase (AKT) (17,33). In the present study, the IKKα/IκBα/NF-κB pathway was examined following treatment with CAN, and it was revealed that p-IKKα and p-IκBα levels were significantly elevated following treatment with CAN. However, IKKα levels were not significantly affected following treatment with CAN. By contrast, total IκBα levels were decreased following treatment with CAN. Other investigations revealed that CAN was a dose-dependent inhibitor of PP2A, resulting in a similar elevation in the phosphorylation of IKKα, AKT and IκBα, thereby regulating the following pathway (18,26,32). The results of the present study confirmed the role of PP2A in the CAN-induced elevation in the phosphorylation of IKKα, AKT and IκBα using a specific activator (DES) of PP2A. Furthermore, in the present study, the IKKα/IκBα/NF-κB pathway was activated and confirmed by the observation of an increased level of p65 in the nucleus and increased phosphorylation levels of p65 in the cells. Numerous studies have demonstrated that activation of the NF-κB pathway may enhance the transcription of a number of genes associated with cell proliferation (14,15,34). However, by contrast, a number of investigations additionally revealed that apoptosis was stimulated by the NF-κB pathway (35). These contradictions may be explained by differences in the cell treatments (35). The results of the present study revealed that CAN inhibited the growth of QBC939 cells by reducing migration and invasion, which was additionally observed in other studies (18,32). Notably, the present study demonstrated that CAN-induced cell inhibition is partially dependent on the activation of the IKKα/IκBα/NF-κB pathway, which was confirmed by inhibition of the nuclear translocation of p65 using an inhibitor (CAPE) of the NF-κB pathway. In addition to this inhibitor, other inhibitors require further investigation to confirm the role of the NF-κB pathway in CAN-induced cell inhibition. Furthermore, in order to fully understand the molecular mechanisms of CAN in cells, further investigation is required.

MMPs are zinc ion-dependent proteases, involved in cell migration and invasion (36,37). Among them, MMP2 and MMP9 are able to degrade the extracellular matrix (ECM) by hydrolyzing collagen IV, through which they promote the migration and invasion of cancer cells into other tissues (37,38). The results demonstrated that the mRNA and protein expression levels of MMP2 and MMP9 were decreased following

treatment of the cells with CAN, which may lead to a decrease in ECM degradation, and inhibition of cell migration and invasion. Notably, studies revealed that NF-κB p65, the subunit of NF-κB, directly activates the expression of MMP2 and MMP9 via interaction with their DNA binding sites (39-41). Previous studies demonstrated that the NF-κB p65 level has a positive association with MMP2 and MMP9 (37,40,42). In addition, studies have reported that activation of the NF-κB pathway promotes tumor cell invasion and migration (43,44). Notably, the results demonstrated that there is a negative association between NF-κB p65, and MMP2 and MMP9, suggesting the inhibitory effects of the NF-κB pathway on cell invasion and migration. TIMPs are the specific inhibitor of MMPs (45-47). Therefore, the expression of MMP2 and MMP9 expression may be implicated in the balance between TIMP-1 and TIMP-2 and NF-κB p65 expression. However, the mechanisms underlying these interactions remain unclear and require further investigation.

In conclusion, following treatment with CAN, cell migration and invasion in the cholangiocarcinoma cell line QBC939 was inhibited. However, the MTT assay revealed that the cytotoxicity of CAN in QBC939 cells was higher compared with HiBECs. The inhibitory effect of CAN on QBC939 cells may partially involve the IKKα/IκBα/NF-κB signaling pathway, and interactions with TIMP-1, TIMP-2, MMP2 and MMP9 proteins.

Availability of data and materials

All data generated and/or analyzed during this study are included in this published article

Authors' contributions

HZ wrote the main manuscript. HZ, JX and SW performed the experiments. HZ and JX designed the study. HZ, SW and JP performed data analysis. JX, SW and JP contributed to manuscript revisions and all authors reviewed the manuscript.

Ethics approval and consent to participate

Not applicable.

Consent for publication

Not applicable.

Competing interests

The authors declare that they have no competing interests.

References

1. Mittal PK, Moreno CC, Kalb B, Mittal A, Camacho JC, Maddu K, Kitajima HD, Quigley BC, Kokabi N and Small WC: Primary biliary tract malignancies: MRI spectrum and mimics with histopathological correlation. Abdom Imaging 40: 1520-1557, 2015.
2. Yang W, Wang X, Zheng W, Li K, Liu H and Sun Y: Genetic and epigenetic alterations are involved in the regulation of TPM1 in cholangiocarcinoma. Int J Oncol 50: 340, 2017.
3. Kim HJ, Kim CY, Hur YH, Koh YS, Kim JC, Kim HJ and Cho CK: The prognostic factors for survival after curative resection of distal cholangiocarcinoma: Perineural invasion and lymphovascular invasion. Surgery Today 44: 1879-1886, 2014.
4. Horie Y, Akamizu Y, Nishimura Y, Maeda N, Kawasaki H, Kimura O, Hirooka Y, Hamazoe R, Kaibara N and Ohta Y: Intrahepatic cholangiocarcinoma with a long-term survival of 12 years after surgical resection: Report of a case and review of the literature. Hepatogastroenterology 42: 506-509, 1995.
5. Yap AQ, Chen CL, Yong CC, Kuo FY, Wang SH, Lin CC, Liu YW, Lin TL, Li WF, Millan CA and Wang CC: Clinicopathological factors impact the survival outcome following the resection of combined hepatocellular carcinoma and cholangiocarcinoma. Surg Oncol 22: 55-60, 2013.
6. Sriputtha S, Khuntikeo N, Promthet S and Kamsa-Ard S: Survival rate of intrahepatic cholangiocarcinoma patients after surgical treatment in Thailand. Asian Pac J Cancer Prev 14: 1107-1110, 2013.
7. Harnois DM, Que FG, Celli A, Larusso NF and Gores GJ: Bcl-2 is overexpressed and alters the threshold for apoptosis in a cholangiocarcinoma cell line. Hepatology 26: 884-890, 1997.
8. Subimerb C, Pinlaor S, Khuntikeo N, Leelayuwat C, Morris A, McGrath MS and Wongkham S: Tissue invasive macrophage density is correlated with prognosis in cholangiocarcinoma. Mol Med Rep 3: 597-605, 2010.
9. Boberg KM, Bergquist A, Mitchell S, Pares A, Rosina F, Broomé U, Chapman R, Fausa O, Egeland T, Rocca G and Schrumpf E: Cholangiocarcinoma in primary sclerosing cholangitis: Risk factors and clinical presentation. Scand J Gastroenterol 37: 1205-1211, 2002.
10. Burak K, Angulo P, Pasha TM, Egan K, Petz J and Lindor KD: Incidence and risk factors for cholangiocarcinoma in primary sclerosing cholangitis. Am J Gastroenterol 99: 523-526, 2004.
11. Purandare NC, Patel II, Trevisan J, Bolger N, Kelehan R, von Bünau G, Martin-Hirsch PL, Prendiville WJ and Martin FL: Biospectroscopy insights into the multi-stage process of cervical cancer development: Probing for spectral biomarkers in cytology to distinguish grades. Analyst 138: 3909-3916, 2013.
12. O'Reilly DA, Roberts JR, Cartmell MT, Demaine AG and Kingsnorth AN: Heat shock factor-1 and nuclear factor-kappaB are systemically activated in human acute pancreatitis. JOP 7: 174-184, 2006.
13. Orban Z, Mitsiades N, Burke TR Jr, Tsokos M and Chrousos GP: Caffeic acid phenethyl ester induces leukocyte apoptosis, modulates nuclear factor-kappa B and suppresses acute inflammation. Neuroimmunomodulation 7: 99-105, 2000.
14. Liacini A, Sylvester J, Li WQ, Huang W, Dehnade F, Ahmad M and Zafarullah M: Induction of matrix metalloproteinase-13 gene expression by TNF-alpha is mediated by MAP kinases, AP-1, and NF-kappaB transcription factors in articular chondrocytes. Exp Cell Res 288: 208-217, 2003.
15. Da Silva-Ferrada E, Torres-Ramos M, Aillet F, Campagna M, Matute C, Rivas C, Rodríguez MS and Lang V: Role of monoubiquitylation on the control of IκBα degradation and NF-κB activity. PLoS One 6: e25397, 2011.
16. Schultze SM, Hemmings BA and Tschopp O: PI3K/AKT, MAPK and AMPK signalling: Protein kinases in glucose homeostasis. Expert Rev Mol Med 14: e1, 2012.
17. Janssens V and Goris J: Protein phosphatase 2A: A highly regulated family of serine/threonine phosphatases implicated in cell growth and signaling. Biochem J 353: 417-439, 2001.
18. Li W, Xie L, Chen Z, Zhu Y, Sun Y, Miao Y, Xu Z and Han X: Cantharidin, a potent and selective PP2A inhibitor, induces an oxidative stress-independent growth inhibition of pancreatic cancer cells through G2/M cell-cycle arrest and apoptosis. Cancer Sci 101: 1226-1233, 2010.
19. Kadioglu O, Kermani NS, Kelter G, Schumacher U, Fiebig HH, Greten HJ and Efferth T: Pharmacogenomics of cantharidin in tumor cells. Biochem Pharmacol 87: 399-409, 2014.
20. Martin WJ, Walton M and Harper J: Resident macrophages initiating and driving inflammation in a monosodium urate monohydrate crystal-induced murine peritoneal model of acute gout. Arthritis Rheum 60: 281-289, 2009.
21. Reddy SB and Patel T: Current approaches to the diagnosis and treatment of cholangiocarcinoma. Curr Gastroenterol Rep 8: 30-37, 2006.
22. Shou LM, Zhang QY, Li W, Xie X, Chen K, Lian L, Li ZY, Gong FR, Dai KS, Mao YX and Tao M: Cantharidin and norcantharidin inhibit the ability of MCF-7 cells to adhere to platelets via protein kinase C pathway-dependent; downregulation of α2 integrin. Oncol Rep 30: 1059-1066, 2013.
23. Imig JD, Dimitropoulou C, Reddy DS, White RE and Falck JR: Afferent arteriolar dilation to 11, 12-EET analogs involves PP2A activity and Ca2+ -activated K + channels. Microcirculation 15: 137-150, 2008.
24. Livak KJ and Schmittgen TD: Analysis of relative gene expression data using real-time quantitative PCR and the 2(-Delta Delta C(T)) method. Methods 25: 402-408, 2001.
25. Tsuchiya Y, Osaki K, Kanamoto M, Nakao Y, Takahashi E, Higuchi T and Kamata H: Distinct B subunits of PP2A regulate the NF-κB signalling pathway through dephosphorylation of IKKβ, IκBα and RelA. FEBS Lett 591: 4083-4094, 2017.
26. Rauh R, Kahl S, Boechzelt H, Bauer R, Kaina B and Efferth T: Molecular biology of cantharidin in cancer cells. Chin Med 2: 8, 2007.
27. Kok SH, Chui CH, Lam WS, Chen J, Lau FY, Cheng GY, Wong RS, Lai PP, Leung TW, Tang JC and Chan AS: Apoptotic activity of a novel synthetic cantharidin analogue on hepatoma cell lines. Int J Mol Med 17: 945-949, 2006.
28. Sharma V, Anderson D and Dhawan A: Zinc oxide nanoparticles induce oxidative DNA damage and ROS-triggered mitochondria mediated apoptosis in human liver cells (HepG2). Apoptosis 17: 852-870, 2012.
29. Zhang L, Li Y, Xing D and Gao C: Characterization of mitochondrial dynamics and subcellular localization of ROS reveal that HsfA2 alleviates oxidative damage caused by heat stress in Arabidopsis. J Exp Bot 60: 2073-2091, 2009.
30. Deng G, Teng Y, Huang F, Nie W, Zhu L, Huang W and Xu H: MicroRNA-101 inhibits the migration and invasion of intrahepatic cholangiocarcinoma cells via direct suppression of vascular endothelial growth factor-C. Mol Med Rep 12: 7079-7085, 2015.
31. He TP, Mo LE and Liang NC: Inhibitory effect of cantharidin on invasion and metastasis of highly metastatic ovarian carcinoma cell line HO-8910PM. Ai Zheng 24: 443-447, 2005 (In Chinese).
32. Hsiao YP, Tsai CH, Wu PP, Hsu SC, Liu HC, Huang YP, Yang JH and Chung JG: Cantharidin induces G2/M phase arrest by inhibition of Cdc25c and Cyclin A and triggers apoptosis through reactive oxygen species and the mitochondria-dependent pathways of A375.S2 human melanoma cells. Int J Oncol 45: 2393-2402, 2014.
33. Martin L, Magnaudeix A, Wilson CM, Yardin C and Terro F: The new indirubin derivative inhibitors of glycogen synthase kinase-3, 6-BIDECO and 6-BIMYEO, prevent tau phosphorylation and apoptosis induced by the inhibition of protein phosphatase-2A by okadaic acid in cultured neurons. J Neurosci Res 89: 1802-1811, 2011.
34. Makarov SS: NF-kappa B in rheumatoid arthritis: A pivotal regulator of inflammation, hyperplasia, and tissue destruction. Arthritis Res 3: 200-206, 2001.
35. Mogi M, Ozeki N, Nakamura H and Togari A: Dual roles for NF-kappaB activation in osteoblastic cells by serum deprivation: Osteoblastic apoptosis and cell-cycle arrest. Bone 35: 507-516, 2004.
36. Jovanović M, Stefanoska I, Radojcić L and Vićovac L: Interleukin-8 (CXCL8) stimulates trophoblast cell migration and invasion by increasing levels of matrix metalloproteinase (MMP)2 and MMP9 and integrins alpha5 and beta1. Reproduction 139: 789-798, 2010.
37. Wu D, Pan H, Zhou Y, Zhou J, Fan Y and Qu P: microRNA-133b downregulation and inhibition of cell proliferation, migration and invasion by targeting matrix metallopeptidase-9 in renal cell carcinoma. Mol Med Rep 10: 2491-2498, 2014.
38. Lo C, Lai TY, Yang JS, Yang JH, Ma YS, Weng SW, Lin HY, Chen HY, Lin JG and Chung JG: Gallic acid inhibits the migration and invasion of A375.S2 human melanoma cells through the inhibition of matrix metalloproteinase-2 and Ras. Melanoma Res 21: 267-273, 2011.

39. Han YP, Tuan TL, Wu H, Hughes M and Garner WL: TNF-alpha stimulates activation of pro-MMP2 in human skin through NF-(kappa)B mediated induction of MT1-MMP. J Cell Sci 114: 131-139, 2001.
40. Prakash M, Kale S, Ghosh I, Kundu GC and Datta K: Hyaluronan-binding protein 1 (HABP1/p32/gC1qR) induces melanoma cell migration and tumor growth by NF-kappa B dependent MMP-2 activation through integrin α(v)β(3) interaction. Cell Signal 23: 1563-1577, 2011.
41. Chen XJ, Wu MY, Li DH and You J: Apigenin inhibits glioma cell growth through promoting microRNA-16 and suppression of BCL-2 and nuclear factor-κB/MMP-9. Mol Med Rep 14: 2352-2358, 2016.
42. Karadimas SK, Klironomos G, Papachristou DJ, Papanikolaou S, Papadaki E and Gatzounis G: Immunohistochemical Profile of NF-κB/p50, NF-κB/p65, MMP-9, MMP-2, and u-PA in experimental cervical spondylotic myelopathy. Spine (Phila Pa 1976) 38: 4-10, 2013.
43. Liu X, Lin R, Zhao B, Guan R, Li T and Jin R: Correlation between oxidative stress and the NF-κB signaling pathway in the pulmonary tissues of obese asthmatic mice. Mol Med Rep 13: 1127-1134, 2016.
44. Wu Y and Zhou BP: TNF-alpha/NF-kappaB/Snail pathway in cancer cell migration and invasion. Br J Cancer 102: 639-644, 2010.
45. Bourboulia D and Stetler-Stevenson WG: Matrix metalloproteinases (MMPs) and tissue inhibitors of metalloproteinases (TIMPs): Positive and negative regulators in tumor cell adhesion. Semin Cancer Biol 20: 161-168, 2010.
46. Bramhall SR, Neoptolemos JP, Stamp GW and Lemoine NR: Imbalance of expression of matrix metalloproteinases (MMPs) and tissue inhibitors of the matrix metalloproteinases (TIMPs) in human pancreatic carcinoma. J Pathol 182: 347-355, 1997.
47. Nagase H and Brew K: Designing TIMP (tissue inhibitor of metalloproteinases) variants that are selective metalloproteinase inhibitors. Biochem Soc Symp 70: 201-212, 2003.